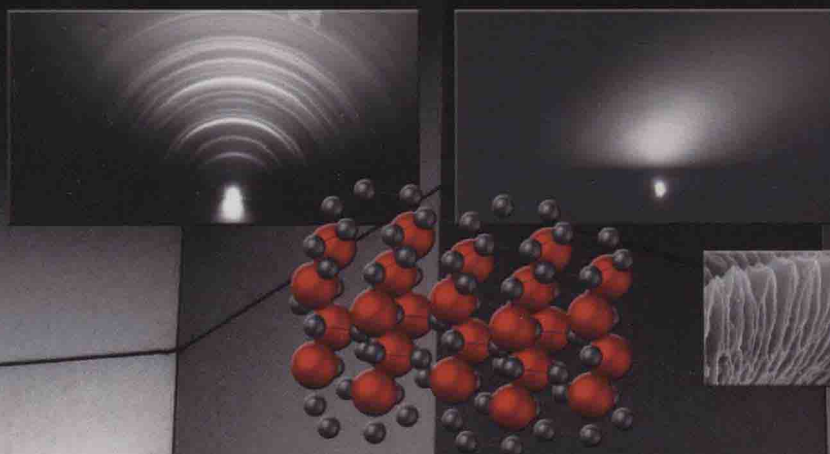


Kirill L. Levine
Editor

Nanoscale-Arranged Systems for Nanotechnology



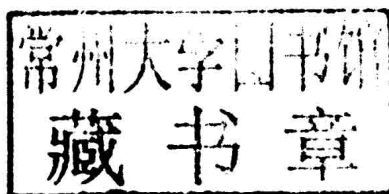
Nanotechnology Science and Technology

NOVA

NANOTECHNOLOGY SCIENCE AND TECHNOLOGY

NANOSCALE-ARRANGED SYSTEMS FOR NANOTECHNOLOGY

KIRILL L. LEVINE
EDITOR



 **nova**
publishers
New York

Copyright © 2015 by Nova Science Publishers, Inc.

All rights reserved. No part of this book may be reproduced, stored in a retrieval system or transmitted in any form or by any means: electronic, electrostatic, magnetic, tape, mechanical photocopying, recording or otherwise without the written permission of the Publisher.

We have partnered with Copyright Clearance Center to make it easy for you to obtain permissions to reuse content from this publication. Simply navigate to this publication's page on Nova's website and locate the "Get Permission" button below the title description. This button is linked directly to the title's permission page on copyright.com. Alternatively, you can visit copyright.com and search by title, ISBN, or ISSN.

For further questions about using the service on copyright.com, please contact:

Copyright Clearance Center

Phone: +1-(978) 750-8400

Fax: +1-(978) 750-4470

E-mail: info@copyright.com.

NOTICE TO THE READER

The Publisher has taken reasonable care in the preparation of this book, but makes no expressed or implied warranty of any kind and assumes no responsibility for any errors or omissions. No liability is assumed for incidental or consequential damages in connection with or arising out of information contained in this book. The Publisher shall not be liable for any special, consequential, or exemplary damages resulting, in whole or in part, from the readers' use of, or reliance upon, this material. Any parts of this book based on government reports are so indicated and copyright is claimed for those parts to the extent applicable to compilations of such works.

Independent verification should be sought for any data, advice or recommendations contained in this book. In addition, no responsibility is assumed by the publisher for any injury and/or damage to persons or property arising from any methods, products, instructions, ideas or otherwise contained in this publication.

This publication is designed to provide accurate and authoritative information with regard to the subject matter covered herein. It is sold with the clear understanding that the Publisher is not engaged in rendering legal or any other professional services. If legal or any other expert assistance is required, the services of a competent person should be sought. FROM A DECLARATION OF PARTICIPANTS JOINTLY ADOPTED BY A COMMITTEE OF THE AMERICAN BAR ASSOCIATION AND A COMMITTEE OF PUBLISHERS.

Additional color graphics may be available in the e-book version of this book.

Library of Congress Cataloging-in-Publication Data

Nanoscale-arranged systems for nanotechnology / editors, Kirill L. Levine, General and Technical Physics, National Mineral Resources University, St. Petersburg, Russia.

pages cm. -- (Nanotechnology science and technology)

Includes index.

ISBN 978-1-63482-353-1 (hardcover)

1. Nanostructured materials. I. Levine, Kirill L.

TA418.9.N35N3443 2015

620'.5--dc23

2015006805

Published by Nova Science Publishers, Inc. † New York

NANOTECHNOLOGY SCIENCE AND TECHNOLOGY

**NANOSCALE-ARRANGED SYSTEMS
FOR NANOTECHNOLOGY**

NANOTECHNOLOGY SCIENCE AND TECHNOLOGY

Additional books in this series can be found on Nova's website
under the Series tab.

Additional e-books in this series can be found on Nova's website
under the e-book tab.

PREFACE

In this research compendium volume of Smart Nanocomposites, various aspects related to nanoscale-arranged systems are discussed. Synthesis, characterization, modeling, and examples of practical usage are in the list of topics brought up in this book. In the discussion are unusual phase transition properties of some oxides, transport properties, electrochemical characterization methods, and optical, electronic, and chemo-sorption properties of nano-structured systems synthesized by various approaches.

NEW MATERIALS

Vanadium dioxide was brought to the focus of research in numerous laboratories because of its intriguing phase transition behavior. Optical information switching in vanadium dioxide and iodine nanoparticles was studied by Khanin and co-workers. Phase transition from metal to semiconductor studied by Ilinsky and co-workers was discussed in terms of electron-related correlation effects responsible for observing phenomena's. Applications in a variety of sensors, super-broad-band transistors, and superfast optical limiters are suggested for those types of structures. Chemosorption in Vanadium dioxide films was described by Tutov with co-workers.

Iodine transport is a tool not only for transferring metals onto surface, but also for implanting them into material, as was shown by Bogdanov. This method also can be used for acceleration of exchange reactions with metals participation.

Low-dimensional oxide systems are another example of nanoscale arranged systems of interest for nanotechnology. Surface lamination and atomic layer deposition methods were described by Ezshovskii. Nanodimensional effects in ponderomotoric interactions, such enhancement in local field strength are discussed in works of Moshnikov and Maksimov.

Electron beam processing was used for the creation of poly(vinylacetate)/graphite nanocomposite with enhanced vibro-absorbing properties, as shown by Mjaking and co-workers.

Continued work on lithium borosilicate glasses coatings with metallic cations was reported by Kashif with co-workers with the emphasis on Infrared spectroscopy as a technique of choice for characterization.

Nano-sized polymer additives for water-based drilling fluids were reported by Manea. Rheological properties of those fluids were evaluated under severe (high pressures, high temperatures) simulated drilling conditions.

DEVICES FOR MEDICAL APPLICATION

Medical aspects, such as targeted drug delivery and photodynamic therapy of cancer, are reflected in publications of Spivak and Vlasenko.

SYNTHETIC METHODS

Among synthetic methods used for nanocomposites preparation, sol-gel is a popular laboratory approach since it is reproducible, cost-effective and diverse, as discussed in paper by Abrashova and co-workers. Precipitation with the help of the surfactant was used to prepare quantum dots in colloidal form. Synthesized nanocrystals were suggested for usage in chemical detection in paper by Mazing and co-workers.

Electrochemical methods remain leaders as a versatile and flexible technique to prepare nanoobjects. By anodic local oxidation reported by Maximov titanium oxide semiconductor was synthesized, while electrochemical anodization of aluminum foil was reported for preparation of anodic porous alumina by Muratova.

MODELLING

Thermodynamical aspects (enthalpy of the formation of intermetallic cadmium tin nanoparticles) were analyzed by Barbin. Approaches to nanostructures characterization by impedance methods were provided in communication by Bezmaternykh and others.

Quantum chemical calculations for titanium oxide nanostructures were reported by Drozdov, while dispersion forces in nanoscale structures of metal-oxide semiconductor were modeled by Lifshitz approach by the group of Fedortsov. Approaches in band modeling of layered semiconductors were addressed by Nemov.

CONTENTS

Preface		vii
Chapter 1	Structural Study of Lithium Borosilicate Glasses Containing Both Iron and Nickel Cations <i>I. Kashif, S. M. Salem, H. Farouk, A. G. Mostafa, Sh. Salem and A. M. Sanad</i>	1
Chapter 2	Surface and Transport Properties of the Phase Change Materials <i>O. S. Komarova, O. A. Martynova, A. V. Babichev, V. E. Gasumyants and S. Vitusevich</i>	13
Chapter 3	Temperature Influence on the Rheology of Water-Based Drilling Fluids with Nano-Sized Polymer Additives <i>Mihaela Manea</i>	21
Chapter 4	Phase and Structure Transitions in Nanoparticles of Semiconductors within Porous Dielectric Matrices <i>S. Khanin, V. Solovyev, S. Trifonov and V. Veisman</i>	29
Chapter 5	Metal Oxide SnO ₂ - ZnO - SiO ₂ Films Prepared by Sol-Gel <i>E. V. Abrashova, I. E. Kononova and V. A. Moshnikov</i>	39
Chapter 6	The Mechanism of Lithium Intercalation into Carbon Graphite Potlining of Aluminium Reduction Cell <i>V. Yu. Bazhin, A. G. Syrkov, R. Yu. Feshchenko and A. V. Saitov</i>	47
Chapter 7	Synthesis of Cadmium Selenide Colloidal Nanoparticles Stabilized with Thioglycolic Acid <i>D. S. Mazing and O. A. Aleksandrova</i>	55
Chapter 8	Investigation of the Optical Properties of Nanoporous Membranes Based on Alumina <i>Ekaterina N. Muratova and Lev B. Matyushkin</i>	63

Chapter 9	Influence of Nanodimensional Effects on Electric Adhesion in Anodic Bonding Manufacturing of Composites Seals <i>N. S. Pshchelko, V. A. Moshnikov and M. P. Sevryugina</i>	71
Chapter 10	Correlation Nature of Phase Transformations in Nanocomposites on the Basis of VO ₂ <i>A. V. Ilinskiy, O. E. Kvashenkina and E. B. Shadrin</i>	79
Chapter 11	Acid-Base Aspect of Control of Nanocomposite Electrical Properties <i>Maxim Sychov, Andrey Syrkov, Yoichiro Nakanishi, Kazuhiko Hara, Hiroko Kominami and Hidenori Mimura</i>	89
Short Communications		97
Chapter 12	Proceedings from the Seminar "Nanophysics and Nanomaterials"	99
Index		177

Chapter 1

STRUCTURAL STUDY OF LITHIUM BOROSILICATE GLASSES CONTAINING BOTH IRON AND NICKEL CATIONS

*I. Kashif, S. M. Salem, H. Farouk, A. G. Mostafa,
Sh. Salem and A. M. Sanad*

Physics Department, Faculty of Science, Al-Azhar University, Cairo, Egypt

ABSTRACT

Glass batches were prepared according to the molecular formula:



where $x = 0.0, 2.5, 5, 7.5, 10$ and 12.5 mol%. In addition a base sample free from Ni and Fe was melted ($35 \text{ Li}_2\text{O} - 31 \text{ B}_2\text{O}_3 - 34 \text{ SiO}_2$).

Both infrared and Mössbauer spectroscopy were used to investigate the structural changes caused by the replacement of nickel by iron cations. The infrared spectra were measured over a continuous spectral range (400 to 2500 cm^{-1}). They show that the replacement of Lithia by nickel oxide decreases the non-bridging oxygen content. Also, the replacement of nickel by iron decreases the concentration of non-bridging oxygens up to 7.5 mol% and then increases it.

From the values of the Mössbauer parameters, all the ferrous cations were found to be in octahedral coordination, while all the ferric ions occupied tetrahedral coordination sites.

The ratio $\{\text{Fe}^{3+} / \sum \text{Fe}_{\text{total}}\}$ increased on replacing nickel by iron up to 7.5 mol % and then became constant. The density increased by replacing nickel by iron up to 7.5 mol% and then decreased.

INTRODUCTION

Infrared and Mössbauer spectroscopy have been extensively employed over the years to investigate the structure of glasses. The alkali - B_2O_3 - SiO_2 ternary glass systems, in particular, have been the subject of numerous infrared studies due to their technological importance. These glasses are used for many applications such as optical glasses, nuclear waste materials and in the electronics industry. In alkali borosilicate glasses with relatively low alkali oxide content, alkali oxide is believed to associate itself with B_2O_3 alone forming an alkali borate phase while SiO_2 forms a silica phase [1-4]. The infrared spectra of these glasses show that alkali oxide is incorporated in the glass to form borate groups such as those found in binary borate glasses [5]. These groups consist of BO_3 and BO_4 units without non-bridging oxygen. The infrared spectra of alkali silicate glasses display a main band at about 1000 cm^{-1} , attributed to the formation of SiO_4 tetrahedra with non-bridging oxygens [6]. Also, the infrared spectra of Na_2O - B_2O_3 - SiO_2 and Al_2O_3 - Na_2O - B_2O_3 - SiO_2 glasses showed bands in the region $1000 - 1120\text{ cm}^{-1}$ arising from the contributions of silicate and borate groups, depending on the concentration of SiO_2 and B_2O_3 [7]. The strongest B - O band in the infrared spectra of Li_2O - B_2O_3 - SiO_2 glasses exists at 1270 cm^{-1} , while for the Si - O band it is at 1060 cm^{-1} [8]. A B - O - Si band was found at 440 cm^{-1} with an intensity mainly a function of composition [9].

The effect of replacing MnO_2 by Fe_2O_3 on the oxidation states of iron in some lithium borosilicate glasses was studied using Mössbauer, infrared and DTA measurements. The Mössbauer spectra showed that the iron ions appeared in the ferric state in both tetrahedral and octahedral coordination and the ratio between the numbers of iron ions in both coordination states did not change with increasing MnO_2 content [10, 11].

The present paper examines the structure of lithium borosilicate glasses containing both iron and nickel cations, in addition to a base sample free from nickel and irons using infrared and Mössbauer spectroscopies, which are valuable tools for the study of amorphous materials. Also, the densities were measured and calculated.

EXPERIMENTAL WORK

Chemically pure oxides were used to prepare the glass batches. The obtained batches, after complete mixing, were melted in platinum crucibles using an electric furnace type (VAF 15/10) LENTON thermal designs at $1200^\circ\text{C} \pm 20^\circ\text{C}$ for two hours. The melts were stirred during melting to ensure complete homogeneity. Then the melt was poured in air on a stainless steel plate, at room temperature. The samples were divided into two parts. One was powdered for the Mössbauer and IR spectroscopy measurements. The other part was used in the solid form for density measurements. The samples were examined using a Philips Analytical X-Ray diffraction system, type PW 3710 with a Cu tube anode. XRD showed no evidence of crystallinity in the quenched glass samples.

The infrared spectra were measured using the KBr disc method and recorded using a JASCO FT/IR 5300 infrared spectrophotometer in the region between 400 and 2500 cm^{-1} .

The Mössbauer spectra of 70mg/cm^2 samples were measured using a constant acceleration spectrometer and a 1.85 GBq, Co^{57} source diffused in chromium matrix. A least square-fitting program based on the line shape distribution was used in order to determine the

Mössbauer parameters. The density of the glass samples was measured at room temperature by the Archimede's technique, with an accuracy up to $\pm 0.0001 \text{ g/cm}^3$. The samples were weighed in air W_a and in a liquid W_l with a known density such as toluene (d_l). Then the density of the samples was calculated using the following formula:

$$d = \{ W_a / (W_a - W_l) \} \times d_l$$

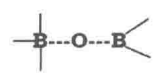
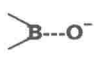
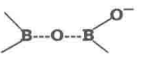

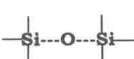
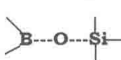
where d is the density of the sample and $d_l = 0.8655 \text{ g/cm}^3$.

RESULTS

Infrared spectra for the glasses melted have been measured and recorded in the region from 400 to 2500 cm^{-1} , to obtain information about changes in the vibration spectra for lithium borosilicate glasses containing different concentrations of NiO and Fe_2O_3 .

Figure (1) shows the IR spectra of the investigated glass samples. The spectrum of the lithium borosilicate glass sample (free from nickel and iron) displayed seven absorption bands, at 1420 , 1030 , 700 , 520 , 500 , 460 and 440 cm^{-1} . And the assignment of the absorption bands detected is summarized in Table 1.

Table 1. The assignment of the absorption bands

Fe - Ni Content	0 - 0	0 - 15	2.5 - 12.5	5 - 10	7.5 - 7.5	10 - 5	12.5 - 2.5	15 - 0**
	1420	1400	1400	1400	1400	1400	1400	1420
	1030	1020	1000	1030	1020	1030	1000	1020
								
	700	700	700	700	700	700	700	740-715
	520	--	540	530	580	---	---	550-500
	460 440	460 430	480	480	480	480	470	475- 460
		410						

** I. Kashif et al. Physics and Chemistry of Glasses 29(1988)72.

When replacing $15\text{mol}\%$ Li_2O by $15\text{mol}\%$ NiO it can be observed that: the two bands at 700 and 460 cm^{-1} are unaffected, and the absorption band at 520 cm^{-1} disappeared. A new absorption band appeared at 410 cm^{-1} , while the bands at 1420 , 1030 and 440 cm^{-1} shifted to lower frequencies at 1400 , 1020 and 430 cm^{-1} respectively.

The molar replacement of NiO by Fe_2O_3 showed that: the absorption bands at 700 and 1400 cm^{-1} were unaffected and appeared in all the investigated glass samples, while the absorption bands at 1020 and 430 cm^{-1} were randomly affected.

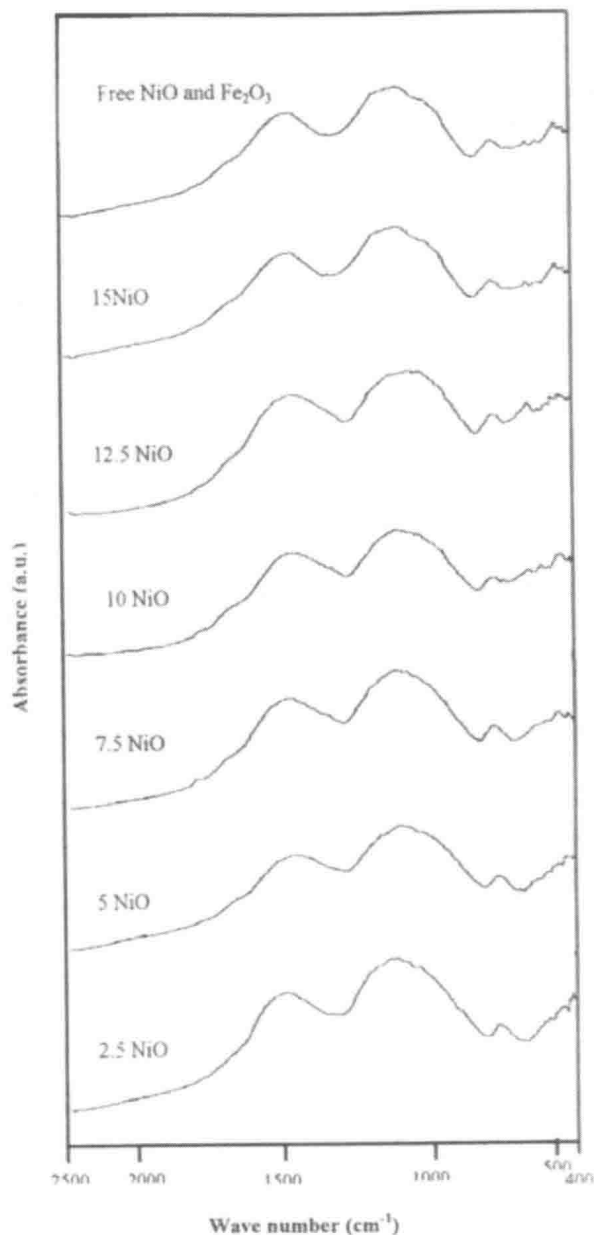
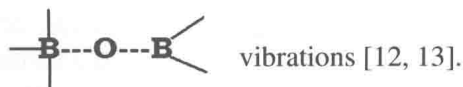
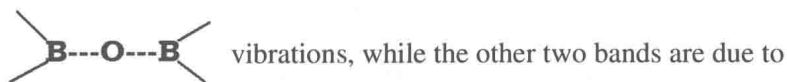


Figure 1. The IR spectra of the investigated glass samples.

The absorption band at 500 cm^{-1} shifted to higher frequencies of 530 and 580 cm^{-1} for the glass samples containing 5 and $7.5\text{ mol\% Fe}_2\text{O}_3$ respectively and then disappeared. The absorption band at 460 cm^{-1} shifted to 480 cm^{-1} for the sample containing $2.5\text{ mol\% Fe}_2\text{O}_3$ and remained constant until the $10\text{ mol\% Fe}_2\text{O}_3$ sample before shifting back to 470 cm^{-1} in the glass sample containing $12.5\text{ mol\% Fe}_2\text{O}_3$.


The infrared spectra of borate glasses show three characteristic absorption bands at 700 , 1260 and 1420 cm^{-1} . The absorption band at 700 cm^{-1} is due to



The addition of Li_2O to the borate glasses gives extra oxygen atoms, which are accommodated into the network, by transferring some boron atoms from triangular BO_3 units to tetrahedral BO_4 units. This could be deduced from the shift of the absorption band at 1420 cm^{-1} to a lower frequency. The vibrations of some boron non-bridging oxygen groups in the form



In the infrared spectrum of the lithium borosilicate glass sample free from NiO and Fe_2O_3 the absorption band at 1420 cm^{-1} may be assigned to $\text{B}-\text{O}$ stretching vibration in two

groups BO_3 and BO_4 , also it may be assigned to . The absorption band at

1030 cm^{-1} is due to stretching vibration of , also it may be attributed to

the contribution of  stretching vibrations [12, 13]. The

bending vibration of  species appears at 460 cm^{-1} [14-16]. The absorption

band at 700 cm^{-1} may be also due to $\text{B}-\text{O}-\text{B}$ bond-bending vibration groups [17, 18]. The fact that all the mentioned bands are broad confirms the vitreous nature of the studied glass samples.

The band that appeared at 520 cm^{-1} is due to $\text{Si}-\text{O}-\text{Si}$ vibrations (19), as well as the bands that appeared at 500 and 440 cm^{-1} which may also be attributed to the bending vibration of $\text{B}-\text{O}$ bonds in a mode involving BO_4 units (17,18) and bending vibration of $\text{Si}-\text{O}$ bonds.

When the nickel oxide was added on the expense of the lithium oxide it was observed that the band at 1420 cm^{-1} shifted to a lower wave number at 1400 cm^{-1} which is attributed to the change of BO_3 to BO_4 units [14-16].

When adding the iron oxide on the expense of the nickel oxide it can be observed that the band that appeared at 1020 cm^{-1} was shifted to a lower frequency with adding the iron oxide at

the expense of nickel oxide up to 7.5 mol% Fe_2O_3 , and then shifted to higher frequency in the glass samples containing more than 7.5 mol% Fe_2O_3 . This indicates that the number of non-bridging oxygen decreased up to 7.5 mol% Fe_2O_3 , and then increased up to 12.5 mol% Fe_2O_3 . The decrease of non-bridging oxygens can be attributed to the substitution of octahedral nickel ions by the largely tetrahedral ferric ions i.e iron ions adopt a network forming role. A new band at 580 cm^{-1} , which appeared in the infrared absorption spectra of the samples containing 2.5, 5, 7.5 mol % Fe_2O_3 , may be due to FeO_6 groups (20). Also the bands that appeared at 430 and 410 cm^{-1} in the spectra of the samples containing 15 mol% NiO and at 420 cm^{-1} in the sample containing 5 mol% Fe_2O_3 may be due to Si – O – S vibrations [11].

The structural changes associated with the nickel and iron addition have been analyzed on the basis of the lithium borosilicate glasses containing two absorption bands related to BO_3 and BO_2O^- triangles and tetrahedral (BO_4^-) groups using spectral de-convolution into their Gaussian components.

From the relative peak areas of BO_3 and BO_2O^- (A_3) and BO_4^- (A_4) peaks, the values of N_4 calculated as $A_4 / (A_4 + A_3)$. The values of N_4 versus Fe_2O_3 content are shown in Figure 2. For all the investigated glass samples, the N_4 values are lower than one, showing the found of BO_3 units in these glass structures. It is well known that in borate glasses there is an isomerization process between three- and four-coordinated boron species as follows:

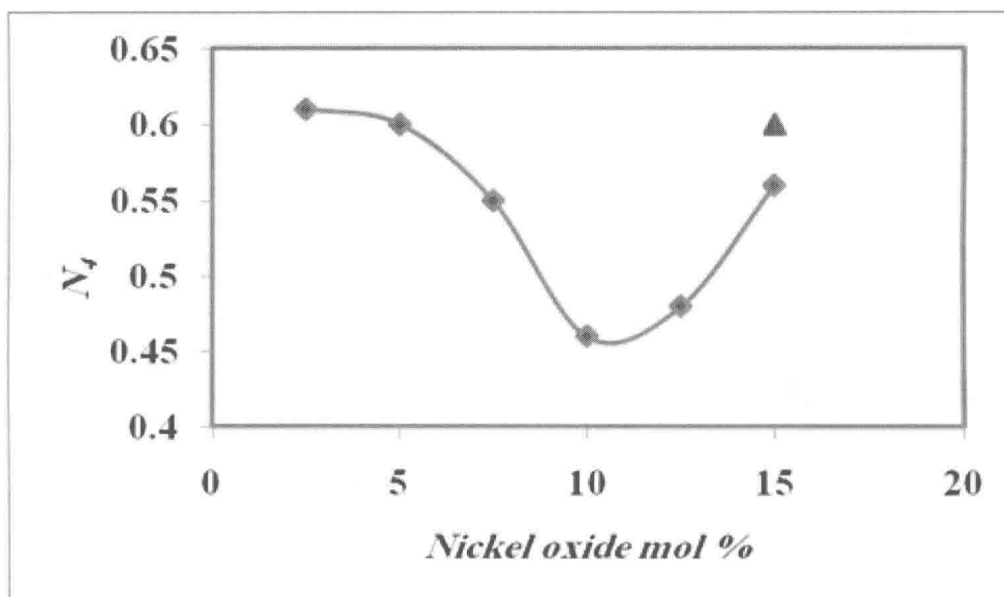


Figure 2. The values of N_4 versus NiO content. ▲ for sample free from Ni and Fe.



The value of N_4 in lithium borosilicate (free from nickel and iron) glass is $N_4 = 0.6$.

The N_4 values are decreased when NiO was introduced into the glass matrix (15 mol %, revealing a kind of equilibrium in the $\text{BO}_4/\text{BO}_3 + \text{BO}_3$ ratio and further modification in the

glasses network, which means that BO_4 units increase. This may be because the oxide ions of Li_2O may be taken up by the NiO to make network forming nickel oxygen structure units, so gradually decreasing the total number of modifier ions and increasing the BO_4 in the networks units.

The N_4 values decreased when the Fe_2O_3 is replaced NiO up to 7.5 mol % and then increased. The decrease of BO_3 can be attributed to the change of coordination of the added ions from the octahedral to the tetrahedral ferric state.

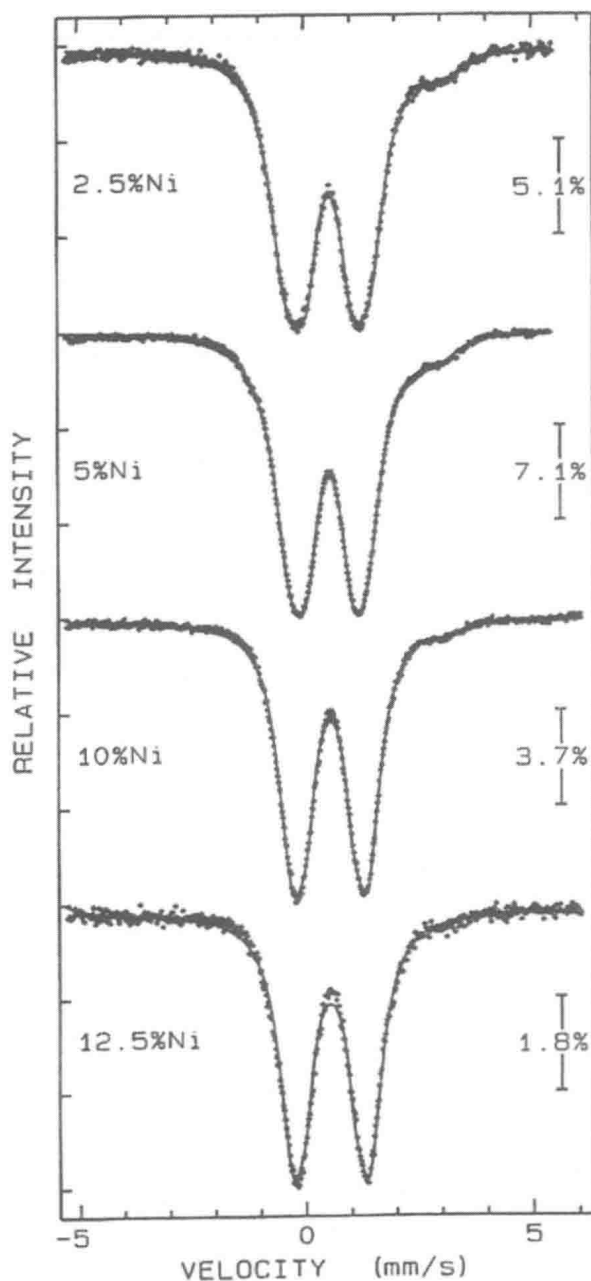


Figure 3. The Mössbauer spectra for the measured samples.

The Mössbauer spectra for the investigated glass samples are represented in Figure (3). The computer analysis indicated that the spectra of the samples containing 2.5, 5 and 7.5 mol% NiO are composed of two paramagnetic doublets, while the spectra of the samples which contain 10 and 12.5 mol% NiO are composed of only one single doublet. It was found that the ferric fraction $\{Fe^{3+}/\sum Fe\}$ increased with the gradual increase of nickel oxide up to 10 mol%, as shown in Figure (4a). The spectra of the samples containing 10 and 12.5 mol% NiO showed no ferrous ions.

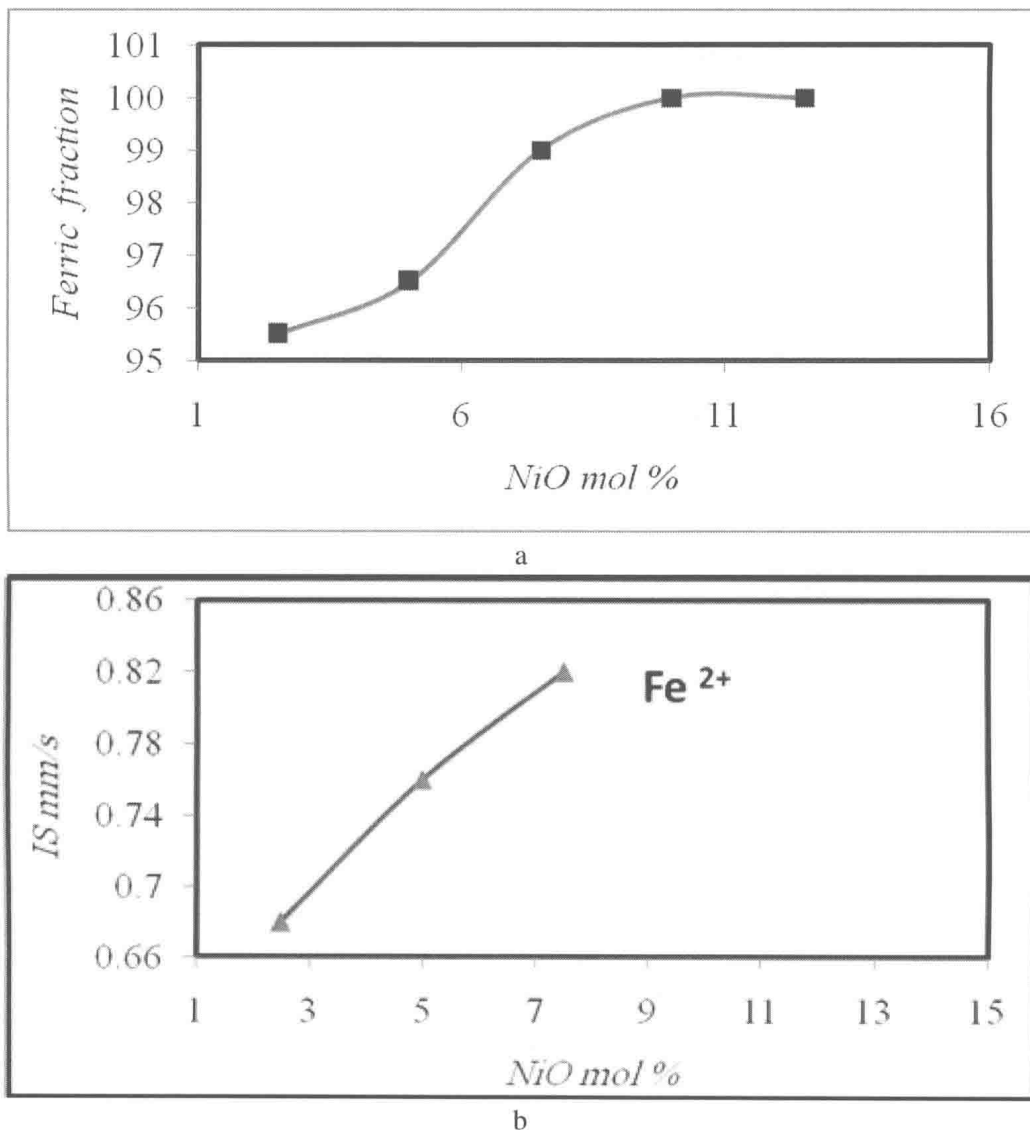


Figure 4. The Mössbauer parameters for the glass samples containing NiO mol% (a) the ferric fraction, (b) the isomer shift (δ).

The changes in the Mössbauer parameters as nickel oxide gradually increased are shown in Figure (4b). The isomer shift (δ) value for Fe^{3+} ions (as a major constituent) appears to increase gradually with the gradual increase of nickel oxide until it reaches a maximum at 7.5